

INFORMATION GEOMETRIC REGULARIZATION OF THE BAROTROPIC EULER EQUATION

RUIJIA CAO* AND FLORIAN SCHÄFER†

Abstract. A key numerical difficulty in compressible fluid dynamics is the formation of shock waves. Shock waves feature jump discontinuities in the velocity and density of the fluid and thus preclude the existence of classical solutions to the compressible Euler equations. Weak “entropy” solutions are commonly defined by viscous regularization, but even small amounts of viscosity can substantially change the long-term behavior of the solution. In this work, we propose an inviscid regularization based on ideas from semidefinite programming and information geometry. From a Lagrangian perspective, shock formation in entropy solutions amounts to inelastic collisions of fluid particles. Their trajectories are akin to that of projected gradient descent on a feasible set of nonintersecting paths. We regularize these trajectories by replacing them with solution paths of interior point methods based on log determinantal barrier functions. These paths are geodesic curves with respect to the information geometry induced by the barrier function. Thus, our regularization amounts to replacing the Euclidean geometry of phase space with a suitable information geometry. We extend this idea to infinite families of paths by viewing Euler’s equations as a dynamical system on a diffeomorphism manifold. Our regularization embeds this manifold into an information geometric ambient space, equipping it with a geodesically complete geometry. Expressing the resulting Lagrangian equations in Eulerian form, we derive a regularized Euler equation in conservation form. Numerical experiments on one and two-dimensional problems show its promise as a numerical tool. While we focus on the barotropic Euler equations for concreteness and simplicity of exposition, our regularization easily extends to more general Euler and Navier-Stokes-type equations.

Key words. Compressible flow, shock waves, interior point methods, information geometry, inviscid regularization, geometric hydrodynamics

MSC codes. 35L65, 76L05, 65M25, 76J20, 58B20

1. Introduction.

1.1. The problem.

The **barotropic Euler equation** describes an inviscid and barotropic gas

$$(1.1) \quad \partial_t \begin{pmatrix} \rho \mathbf{u} \\ \rho \end{pmatrix} + \operatorname{div} \begin{pmatrix} \rho \mathbf{u} \otimes \mathbf{u} + P(\rho) \mathbf{I} \\ \rho \mathbf{u} \end{pmatrix} = \begin{pmatrix} \mathbf{f} \\ 0 \end{pmatrix}.$$

Here, $\mathbf{u}(\mathbf{x}, t)$ denotes the velocity of a gas particle passing through a point \mathbf{x} at time t and $\rho(\mathbf{x}, t)$ denotes the gas density in \mathbf{x} at t . Thus, $\boldsymbol{\mu}(\mathbf{x}, t) = \rho(\mathbf{x}, t)\mathbf{u}(\mathbf{x}, t)$ denotes the momentum density in \mathbf{x} at time t . By the barotropic assumption, the pressure P depends only on the density, \mathbf{f} denotes external forces acting on the gas.

Shock formation in compressible flows. The steepening of wavefronts is characteristic of compressible flows. It arises from faster upstream particles catching up to slower downstream ones, steepening the slope of \mathbf{u} and forming singular shocks. Shock formation was proved for a wide range of flows [54, 20, 18, 21, 19].

Vanishing viscosity solutions and entropy conditions. Shock waves preclude long-term existence of classical solutions to (1.1). The canonical solution concept are limits of Navier Stokes solutions with vanishing viscosity or refinements thereof [33](see Figure 1). They are also characterised by entropy conditions (see, e.g. [41]).

*Georgia Tech (rcao62@gatech.edu).

†Georgia Tech (fts@gatech.edu).

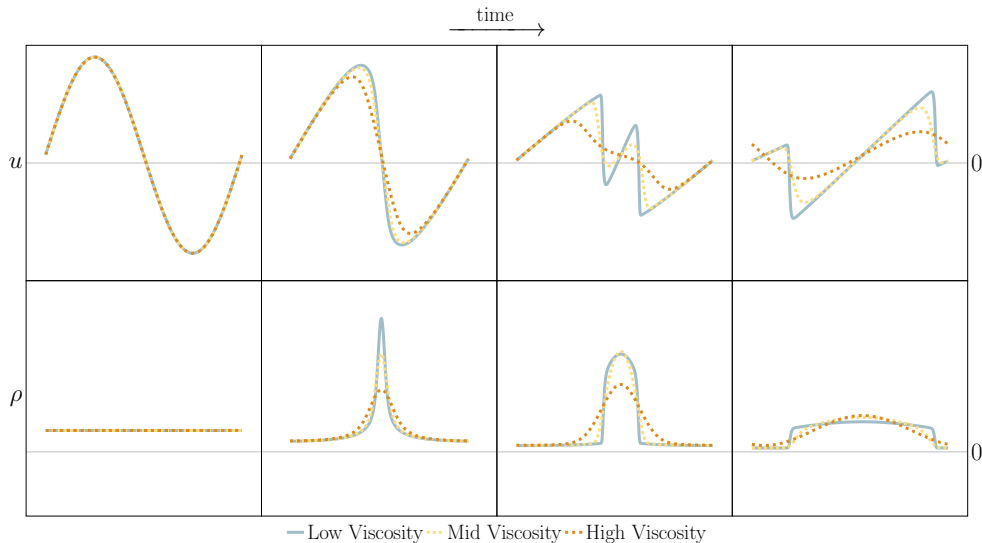


FIG. 1. *Vanishing viscosity solutions.* In the presence of shocks, solutions are defined as the limit of solutions obtained with decreasing viscosity. For any given viscosity, the solution becomes excessively smooth over time.

1.2. Existing approaches.

Localized viscosity. Naive approaches for computing viscosity solutions require a mesh width proportional to the viscosity parameter, leading to excessive computational cost or energy dissipation. Instead, numerous methods add viscosity *adaptively*, according to shock indicators [56, 50, 23, 27, 45, 8, 32, 15, 24].

Purely numerical remedies emphasize the avoidance of Gibbs oscillations encountered by high-order schemes near shocks using limiters that reduce the approximation order at the shock [55, 51] and (W)ENO-type schemes that select the reconstruction stencil adaptively [43, 34, 53]. The numerical dissipation of low-order methods result in behavior similar to localized viscosity. However, a downside of these methods is the absence of a well-defined PDE. For instance, stencil-switching and slope limiters introduce errors in adjoint-based sensitivities [13, 44].

Inviscid PDE-based regularization. A third line of work aims to develop *inviscid* PDE-based regularizations. First attempts based on [40] failed to capture the correct shock speeds of the Euler equations, making them unsuitable for most applications [12, 11, 10]. [31] proposes inviscid nondispersive regularizations based on [22]. It maintains the correct shock speed but is limited to unidimensional problems.

1.3. This work.

Interior point methods for Euler. For vanishing P, \mathbf{f} , (1.1) reduces to Burgers' equation, solvable by the method of characteristics. Shocks form when characteristics meet. Viscosity solutions follow solution paths of projected gradient descent under the constraint of non-crossing characteristics. This work modifies characteristics to follow solution paths of interior point methods defined by a barrier ψ [46]. This ensures strict feasibility (avoidance of shocks) while preserving long-term behavior.

Information geometry on diffeomorphism manifolds. To make this idea precise, we use the fact that solution paths of interior point methods are dual geodesics in the information geometry defined by ψ [2, 1]. Collectively, Burgers characteristics describe geodesics on diffeomorphism manifolds [6, 25, 38, 39]. Our regularization replaces them with dual geodesics in the information geometry of ψ . Adding forces of \mathbf{f}, P and returning to a Eulerian description results in the regularized Euler equation

$$(1.2) \quad \begin{cases} \partial_t \begin{pmatrix} \rho u \\ \rho \end{pmatrix} + \operatorname{div} \begin{pmatrix} \rho u \otimes u + P(\rho)\mathbf{I} + \mathbf{F} \\ \rho u \end{pmatrix} = \begin{pmatrix} \mathbf{f} \\ 0 \end{pmatrix} \\ \rho^{-1}\mathbf{F} - \alpha D(\rho^{-1} \operatorname{div} \mathbf{F}) = 2\alpha[D\mathbf{u}][D\mathbf{u}]. \end{cases}$$

This work focuses on the barotropic Euler equations for concreteness and to simplify the exposition. But one can easily derive extensions to general Euler and Navier-Stokes-type equations by adding the regularization term \mathbf{F} to their momentum flux. By choosing $\sqrt{\alpha}$ proportional to the mesh size, the elliptic problem defining \mathbf{F} in (1.2) can be solved efficiently by a constant number of Jacobi or Gauss-Seidel iterations.

2. Information geometric regularization.

2.1. A Lagrangian view on shock formation.

Model problem: The Burgers equation. For simplicity, we illustrate our approach on the unidimensional case of equation (1.1), with $P, \mathbf{f} \equiv 0$.

$$(2.1) \quad \partial_t \begin{pmatrix} \rho u \\ \rho \end{pmatrix} + \partial_x \begin{pmatrix} \rho u^2 \\ \rho u \end{pmatrix} = \begin{pmatrix} 0 \\ 0 \end{pmatrix}.$$

By combining the two equations, a brief calculation yields the Burgers' equation

$$(2.2) \quad \partial_t \begin{pmatrix} u \\ \rho \end{pmatrix} + \partial_x \begin{pmatrix} u^2/2 \\ \rho u \end{pmatrix} = \begin{pmatrix} 0 \\ 0 \end{pmatrix}.$$

The second equation is often discarded and the Burgers equation written as

$$(2.3) \quad \partial_t u + u \partial_x u = 0.$$

Smooth solutions of (2.2) describe the inertial movement of noninteracting particles.

Characteristics and shock formation. Burgers' equation is solvable by the methods of characteristics [26]. For initial conditions $u(\cdot, 0)$ and a family of curves

$$\Phi_t(x) := x + tu(x, 0), \quad \text{define the solution } u \text{ as } u(\Phi_t(x), t) := u(x, 0).$$

The solution in (x, t) is obtained by tracing the line $\{\Phi_t(y)\}$ passing through x at time t to the initial condition. If y is unique, u satisfies Burgers' equations, since

$$0 = \frac{d}{dt} (u(\Phi_t(x), t)) = \left[\partial_t u + \partial_x \left(\frac{u^2}{2} \right) \right] (\Phi_t(x), t).$$

The characteristic curve $t \mapsto \Phi_t(x)$ describes the trajectory of a particle with initial position x and velocity $u(x, 0)$. As shown in Figure 2, shocks in the Burgers equation form when characteristic curves cross and thus the solution can not be traced back to a unique initial condition. Physically, this amounts to collision of particles. In a vanishing viscosity solution, characteristics of colliding particles merge to continue with their average velocity. Thus, particle collisions in vanishing viscosity solutions of the Burgers equation are fully inelastic (see Figure 3).

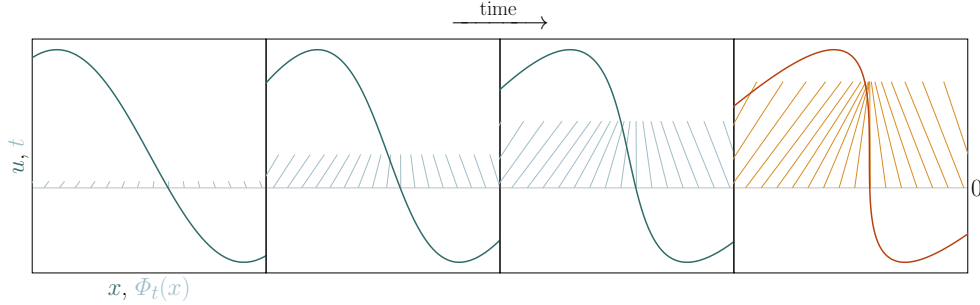


FIG. 2. **Shock formation and characteristics.** The plot overlays the Burgers' characteristics with the velocity profile, at four different time steps. As the characteristics approach each other, the profile steepens. In the rightmost plot, the characteristics cross and the flow develops a shock.

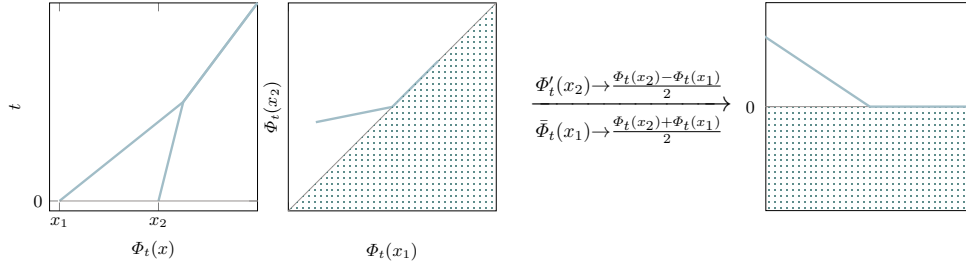


FIG. 3. **Collision of Characteristics.** When Burgers' characteristics cross, they merge and a shock forms. In phase space, this means that the system evolves on the boundary of the feasible set that is accessible without crossing characteristics. In transformed coordinates, it is a half-space.

2.2. Semidefinite programming meets fluid dynamics.

Interior point methods for Euler. Shock formation occurs when characteristics meet. We examine trajectories $t \mapsto (\Phi_t(x_1), \Phi_t(x_2))$ of two characteristics initialized in x_1 and x_2 . **Figure 3** shows the feasible region \mathcal{R} in phase space where shocks do not form. In coordinates $\bar{\Phi}_t = (\Phi_t(x_1) + \Phi_t(x_2))/2$ and $\Phi'_t = (\Phi_t(x_1) - \Phi_t(x_2))/2$, the feasible region \mathcal{R} becomes the positive half space. When reaching the boundary $\partial\mathcal{R}$, a shock forms and the merged characteristics continue on $\partial\mathcal{R}$. This is the solution path of projected gradient ascent on $\max_{\mathbf{v} \in \mathcal{R}} \langle \mathbf{u}_{t=0}(x_1, x_2), \mathbf{v} \rangle$ [16]. In contrast to projection-based approaches, interior point methods maintain strict feasibility of iterates. They add a barrier function to the objective and slowly decrease its weight to zero. For positive (semidefinite) programming, $-\log(\det)$ is a popular choice [46, 47]. This work develops interior point methods for Euler equations that maintain feasibility (regularity) while preserving the long-time behavior of the solution.

Information geometric regularization. The negative log-determinant barrier function of semidefinite programming is also the negative entropy of the family of centered Gaussians, interpreting the optimization variable as a covariance matrix. As such, it defines a *dually flat information geometry* on the cone of positive-definite matrices [5, 1, 7]. The Hessian of the barrier function is the Riemannian metric while its gradient defines a notion of straight line [48, 1]. These so-called *dual geodesics*

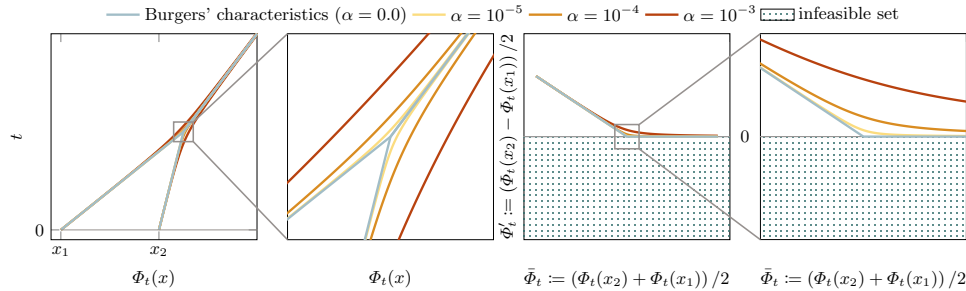


FIG. 4. **Geometric regularization.** Regularizing the $\bar{\Phi}$ - Φ' geometry of a pair of characteristics with the barrier term $\alpha(-\log(\Phi'))$ avoids shock formation while preserving the long-time behavior.

are neither straight lines in the ordinary sense, nor are they minimizing the length defined by the Riemannian metric. However, they have the property of *bending away* from the boundary of the positive-definite cone, preserving feasibility. By the same construction, any convex barrier function ψ induces a dually flat geometry. For a linear objective function $\mathbf{x} \mapsto \mathbf{v}^T \mathbf{x}$, the iterates of interior point methods with barrier function ψ move along such a dual geodesic [1, Chapter 13.5] in the direction \mathbf{v} . Using the barrier function ψ thus amounts to replacing ordinary straight lines with dual geodesics generated by ψ . This perspective extends beyond optimization problems and applies to characteristics of the Burgers equation, which are Euclidean straight lines in $(\bar{\Phi}, \Phi')$ -space. Euclidean straight lines are dual geodesics of

$$\psi_E(\bar{\Phi}) := \psi_E(\bar{\Phi}, \Phi') := \frac{\bar{\Phi}^2 + \Phi'^2}{2} = \frac{\Phi(x_1)^2 + \Phi(x_2)^2}{2}.$$

Information geometric regularization modifies the Burgers and Euler equations by changing ψ to account for the positivity constraint on Φ' . For instance, we can choose

$$\psi(\bar{\Phi}) := \psi(\bar{\Phi}, \Phi') := \psi_E + \alpha(-\log(\Phi')),$$

where $\alpha \geq 0$ modulates the regularization. Figure 4 shows how the resulting characteristics approach the boundary of the feasible sets, without leaving it.

2.3. Information Geometry in the infinite-dimensional setting.

From characteristics to diffeomorphisms. To obtain a Eulerian description of the modified equation, we have to extend the construction in Figure 4 from two characteristics to an infinity of characteristics. Instead of keeping track of individual characteristics of the form $t \mapsto \Phi_t(x)$, we keep track of the path $t \mapsto \Phi_t$ in function space. Beginning with the seminal work of Arnold, the field of geometric hydrodynamics has studied fluid dynamics as geodesic curves on diffeomorphism manifolds [6]. Arnold, Ebin, and Marsden focused on inviscid and incompressible fluids that are described by geodesics on the manifold of volume-preserving diffeomorphisms [6, 25]. Similarly, the inviscid Burgers' and compressible Euler equations are solutions of the geodesic or Newton equations with respect to the L^2 metric on the manifold of general (not necessarily volume preserving) diffeomorphisms [38, 39]. This manifold is not geodesically complete under the L^2 metric, meaning some L^2 geodesics cannot continue indefinitely before leaving the manifold of diffeomorphisms. As $t \mapsto \Phi_t$ reaches

the boundary of the manifold, its spatial derivative $D\bar{\Phi} := \partial_x \bar{\Phi}$ becomes singular and $\bar{\Phi}$ ceases to be differentiably invertible. In physical terms, the flow develops a shock.

Regularization on the diffeomorphism manifold. The regularization of geodesic curves of diffeomorphisms is analogous to that of characteristic curves as shown in [Figure 4](#). For characteristic curves, new coordinates $(\bar{\Phi}, \bar{\Phi}')$ are obtained by $\bar{\Phi} = (\Phi(x_1) + \Phi(x_2))/2$ and $\bar{\Phi}' = (\Phi(x_1) - \Phi(x_2))/2$. For diffeomorphisms, we define $\bar{\Phi} := \int_{\mathbb{R}} (\Phi(x) - x) dx$ and $\bar{\Phi}' := \partial_x \bar{\Phi}$, with the latter being function-valued. The Euclidean barrier is $\psi_E := \frac{1}{2} \|\bar{\Phi}(\cdot) - (\cdot)\|_{L^2}^2$, yielding the modified barrier

$$(2.4) \quad \psi(\Phi) = \psi_E(\Phi) + \alpha \int_{\mathbb{R}} (-\log(\partial_x \bar{\Phi})) dx.$$

Integration amounts to summing infinitely many barrier functions, each preventing a pair of characteristics from crossing, akin to the universal barrier function of [\[46\]](#).

2.4. From Burgers to Euler: The final equations.

A barrier function for volume forms. Positivity of $\partial_x \bar{\Phi}$ for equations on \mathbb{R} extends to positivity of the Jacobian determinant $\det(D\bar{\Phi})$ for equations on \mathbb{R}^d . This motivates using the log determinant barrier function of positive-definite programming,

$$(2.5) \quad \psi(\Phi) = \psi_E(\Phi) + \alpha \int_{\mathbb{R}^d} (-\log \det(D\bar{\Phi})) dx.$$

Although $-\log \det$ is only convex on symmetric-positive matrices, ψ is geodesically convex on the diffeomorphisms manifold, making it a valid barrier function that generalizes information geometric regularization to the multidimensional case.

Pressure and external forces. Whereas Burgers' equation and its multidimensional analogs are geodesic equations on the diffeomorphism manifold, the compressible Euler and Navier-Stokes equations arise by adding forces to the geodesic equations [\[39\]](#), due to pressure, viscosity, and external forces acting on the gas. Adding these forces to dual geodesic equations yields regularizations of the Euler and Navier Stokes equations and numerous other systems including those listed in [\[39, Table 1\]](#). For the sake of concreteness, this work focuses on the case of the barotropic Euler equation.

Euclidean description. We obtain the final regularized equation by converting the Lagrangian representation in terms of diffeomorphism maps $\bar{\Phi}$ to a Eulerian description in terms of ρ and $\rho \mathbf{u}$ using $\mathbf{u}(\bar{\Phi}(x)) := \dot{\bar{\Phi}}(x)$ and $\rho(\bar{\Phi}(x)) := (\det(D\bar{\Phi}))^{-1}$. Using these definitions, we also note that $\int_{\mathbb{R}^d} -\log \det(D\bar{\Phi}) dx = \int_{\mathbb{R}^d} \log(\rho) \rho dx$. The regularization term is the negative Shannon entropy of the particle distribution.

3. Deriving the modified equations.

3.1. Derivation with general barrier function.

3.1.1. Notation and Setting. We begin by deriving information geometric regularization for a general barrier function ψ . Since a formal derivation is sufficient to obtain the regularized PDE, we will not discuss the various technical complications that arise in the treatment of infinite-dimensional manifolds, as discussed in [\[52\]](#). We restrict the derivation to flows on \mathbb{R}^d decaying at infinity and postpone the treatment of bounded domains and boundary values to future work. Using the ambient space $\mathcal{A} := \mathbf{I} + H^1(\mathbb{R}^d; \mathbb{R}^d)$, we denote as $\mathcal{M} \subset \mathcal{A}$ the diffeomorphism manifold, where

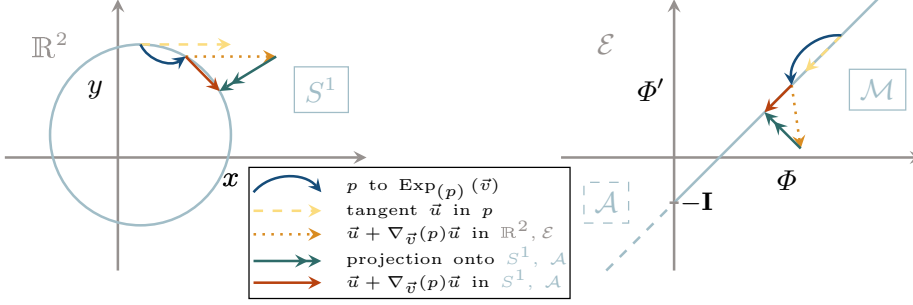


FIG. 5. **Parallel transport on \mathcal{A} :** Parallel transport on $S^1 \hookrightarrow \mathbb{R}^2$ amounts to parallel transport in \mathbb{R}^2 followed by projection onto TS^1 . Parallel transport on $\mathcal{A} \hookrightarrow \mathcal{E}$ is computed similarly but now the embedded manifold \mathcal{A} instead of the embedding manifold \mathcal{E} is flat in canonical coordinates.

\mathbf{I} denotes the identity function on \mathbb{R}^d . We consider \mathcal{A} as an affine subspace of the extended ambient space $\mathcal{E} := (\mathbf{I} + L^2(\mathbb{R}^d; \mathbb{R}^d)) \times (\mathbf{I} + L^2(\mathbb{R}^d; \mathbb{R}^{d \times d}))$ through the embedding $\Phi \mapsto (\Phi, D\Phi)$. We denote by capital Greek letters points on the manifolds \mathcal{M} , \mathcal{A} , and \mathcal{E} and by capital Roman letters the elements of their tangent spaces. We denote elements of \mathcal{E} or its tangent spaces as (Φ, Φ') or (U, U') to distinguish the two degrees of freedom.

3.1.2. The information geometry on the extended ambient space. We begin by defining a dually flat geometry on the extended ambient space \mathcal{E} . For $\psi : \mathcal{E} \rightarrow \mathbb{R}$ convex, we define a Riemannian metric through its Hessian operator

$$(3.1) \quad \langle (U, U'), (V, V') \rangle_{(\Phi, \Phi')} := \langle (U, U'), [D^2\psi(\Phi, \Phi')] (V, V') \rangle_{L^2}.$$

Euclidean geodesics are straight lines in \mathcal{E} , of the form

$$(3.2) \quad (\Phi_t, \Phi'_t) = \text{Exp}_{(\Phi_0, \Phi'_0)}(tU, tU') := (\Phi_0, \Phi'_0) + t(U, U').$$

$\text{Exp}_{(\Phi, \Phi')}(U, U')$ denotes the exponential map at (Φ, Φ') in direction (U, U') . In dually flat spaces [1], these *primal* geodesics are complemented by *dual* geodesics of the form

$$(3.3) \quad (\Phi_t, \Phi'_t) = \text{Exp}_{(\Phi_0, \Phi'_0)}^\psi(tU, tU') := \nabla\psi^{-1}(\nabla\psi(\Phi_0, \Phi'_0) + t[D^2\psi(\Phi_t, \Phi'_t)](U, U')),$$

where $\text{Exp}_{(\cdot)}^\psi(\cdot)$ denotes the dual exponential map of induced by ψ . Dual geodesics are Euclidean straight lines after transforming \mathcal{E} with $\nabla\psi$, motivating the term dually flat geometry. The coordinate system given by $\nabla\psi$ defines a covariant derivative as

$$\begin{aligned} [\nabla_{V, V'}(\Phi, \Phi')](U, U') &:= \left. \frac{d}{ds} \right|_{s=0} [D^2\psi(\Phi + sV, \Phi' + sV')]^{-1} [D^2\psi(\Phi, \Phi')](U, U') \\ &= - [D^2\psi(\Phi, \Phi')]^{-1} \left. \frac{d}{ds} \right|_{s=0} [D^2\psi(\Phi + sV, \Phi' + sV')](U, U') \\ &= - [D^2\psi(\Phi, \Phi')]^{-1} [D^3\psi(\Phi, \Phi')]((U, U'), (V, V')), \end{aligned}$$

where we interpret $[D^3\psi(\Phi, \Phi')]$ as a map from $\mathcal{E} \times \mathcal{E}$ to \mathcal{E} .

3.1.3. Parallel transport on \mathcal{A} . We use the embedding $\mathcal{A} \hookrightarrow \mathcal{E}$ to derive a dual exponential map on \mathcal{A} from that defined on \mathcal{E} . Even if (Φ_0, Φ'_0) is contained in \mathcal{A} and (U, U') in its tangent space, their image under the dual exponential map need not be contained in \mathcal{A} . The covariant derivative is not contained in the tangent space, thus “pointing out of the submanifold.” This is akin to the situation in Euclidean space where straight lines tangential to a submanifold are not usually contained in that manifold (see Figure 5). In both cases, projecting the result of the parallel transport in the embedding space back onto the tangent space of the embedded manifold defines a covariant derivative on it. The resulting covariant derivative on \mathcal{A} is

$$(3.4) \quad [\nabla_V(\Phi)](U) = \arg \min_{W \in H^1} \|(W, DW) - [\nabla_{V, V'}(\Phi, \Phi')](U, U')\|_{(\Phi, D\Phi)}^2,$$

with $\|\cdot\|_{(\Phi, D\Phi)}$ the norm induced by the Riemannian metric $\langle \cdot, \cdot \rangle_{\Phi, D\Phi}$.

3.1.4. The regularized geodesic equation. The dual covariant derivative on \mathcal{A} defines geodesic equations (subject to a force \mathbf{k}) as curves $t \mapsto \Phi_t$ satisfying

$$(3.5) \quad [\nabla_{\dot{\Phi}_t}(\Phi)]((\dot{\Phi}_t)) + \mathbf{k} = \ddot{\Phi}_t.$$

The deformation maps of the Burgers and Euler equations under an external force \mathbf{f} satisfy this geodesic equation using the primal covariant derivative and $\mathbf{k} \equiv -\mathbf{f}$ and $\mathbf{k} \equiv \nabla P - \mathbf{f}$, respectively [38, 39]. We propose their modification by replacing the primal with the dual covariant derivative, which we now derive explicitly.

Remark 3.1. As described in [39], the Euler equations can also be considered as Newton equations with a potential given by the internal energy $\Phi \mapsto E(\Phi)$. It seems natural to attempt to instead take the gradient of the potential with respect to the metric defined by ψ , but numerical evidence suggests that this greatly alters the behavior of the resulting equation, limiting its practical utility.

3.2. The unidimensional case using the log barrier. We use the potential ψ on \mathcal{E} , defined as

$$\psi(\Phi, \Phi') := \frac{1}{2} \int_{\mathbb{R}} \|\Phi(x)\|^2 dx + \alpha \int_{\mathbb{R}} -\log(\Phi'(x)) dx.$$

3.2.1. Unidimensional case, Lagrangian description. The derivative map is given by

$$[D\psi(\Phi, \Phi')](V, V') = \int_{\mathbb{R}} \Phi(x)V(x) dx + \alpha \int_{\mathbb{R}} -\frac{V'(x)}{\Phi'(x)} dx$$

and thus the gradient map (with respect to the L^2 metric) is given by

$$\nabla\psi(\Phi, \Phi') = \left(\Phi, -\alpha(\Phi')^{-1} \right),$$

which is its own inverse. The Hessian quadratic form is given by

$$(3.6) \quad [D^2\psi(\Phi, \Phi')](U, U'), (V, V') = \int_{\mathbb{R}} U(x) \cdot V(x) dx + \alpha \int_{\mathbb{R}} \frac{\partial_x U(x) \cdot \partial_x V(x)}{(\Phi'(x))^2} dx.$$

Together with the L^2 inner product, it defines a linear mapping from \mathcal{E} to itself as

$$[D^2\psi(\Phi, \Phi')] (U, U') = \left(U(x), \alpha \frac{U'(x)}{(\Phi'(x))^2} \right).$$

We now compute the cubic form given by third order derivatives

$$[D^3\psi(\Phi, \Phi')] ((U, U'), (V, V'), (W, W')) = -2\alpha \int_{\mathbb{R}} \frac{U'(x) \cdot V'(x) \cdot W'(x)}{(\Phi'(x))^3} dx.$$

Again using the L^2 inner product, we can write this as a mapping from $\mathcal{E} \times \mathcal{E}$ to \mathcal{E} .

$$[D^3\psi(\Phi, \Phi')] ((U, U'), (V, V')) = \left(0, -2\alpha \frac{U'(x) \cdot V'(x)}{(\Phi'(x))^3} \right).$$

Plugging these computations into (3.4), we obtain covariant derivatives on \mathcal{A} , \mathcal{M} as (3.7)

$$[\nabla_{V, V'}(\Phi, \Phi')] (U, U') = \arg \min_{W \in T_{\Phi} \mathcal{M}} \int_{\mathbb{R}} \|W(x)\|^2 dx + \alpha \int_{\mathbb{R}} \frac{\left\| \partial_x W - 2 \frac{\partial_x U(x) \cdot \partial_x V(x)}{(\partial_x \Phi(x))} \right\|^2}{(\partial_x \Phi(x))^2} dx.$$

Taking a variation $\delta W \in T_{\Phi} \mathcal{M} = H^1(\mathbb{R})$, we obtain

$$(3.8) \quad \int W(x) \delta W(x) + \alpha \frac{\left(\partial_x W(x) - 2 \frac{\partial_x U(x) \cdot \partial_x V(x)}{(\partial_x \Phi(x))} \right) \partial_x \delta W(x)}{(\partial_x \Phi(x))^2} dx = 0.$$

Thus, W satisfies the divergence form elliptic PDE

$$(3.9) \quad -\alpha \partial_x \left(\frac{\partial_x W(x)}{(\partial_x \Phi(x))^2} \right) + W(x) = -\alpha \partial_x \left(\frac{2 \partial_x U(x) \cdot \partial_x V(x)}{(\partial_x \Phi(x))^3} \right).$$

We can now plug this formula for the covariant derivative into the geodesic equation

$$(3.10) \quad \left[\nabla_{(\dot{\Phi}, \partial_x \dot{\Phi})} (\Phi, \partial_x \Phi) \right] (\dot{\Phi}, \partial_x \dot{\Phi}) = (\ddot{\Phi}, \partial_x \ddot{\Phi}).$$

The resulting equation, still in Lagrangian coordinates, is given by

$$(3.11) \quad -\alpha \partial_x \left(\frac{\partial_x \ddot{\Phi}(x)}{(\partial_x \Phi(x))^2} \right) + \ddot{\Phi}(x) = -2\alpha \partial_x \left(\frac{\partial_x \dot{\Phi}(x) \cdot \partial_x \dot{\Phi}(x)}{(\partial_x \Phi(x))^3} \right).$$

3.3. Unidimensional case, Eulerian description. We now transfer the geodesic equation into Eulerian coordinates. Define u as

$$(3.12) \quad \dot{\Phi}(x) =: u(\Phi(x)) \quad \Rightarrow \quad \ddot{\Phi}(x) = u(\Phi(x)) \partial_x u(\Phi(x)) + \partial_t u(\Phi(x)).$$

Plugging this ansatz into the equations, we obtain

$$(3.13) \quad -\alpha \partial_x \left(\frac{\partial_x (u \partial_x u + \partial_t u) \circ \Phi}{\partial_x \Phi(x)} \right) + (u \partial_x u + \partial_t u) \circ \Phi = -2\alpha \partial_x \left(\frac{(\partial_x u)^2 \circ \Phi}{\partial_x \Phi(x)} \right).$$

We multiply with a test $x \mapsto w \circ \Phi$ and integrate

$$(3.14) \quad - \int_{\mathbb{R}} w \circ \Phi \cdot \alpha \partial_x \left(\frac{\partial_x (u \partial_x u + \partial_t u) \circ \Phi}{\partial_x \Phi(x)} \right) + \int_{\mathbb{R}} w \circ \Phi \cdot (u \partial_x u + \partial_t u) \circ \Phi \, dx$$

$$(3.15) \quad = - \int_{\mathbb{R}} w \circ \Phi \cdot 2\alpha \partial_x \left(\frac{(\partial_x u)^2 \circ \Phi}{\partial_x \Phi(x)} \right) \, dx.$$

Via integration by parts on RHS and the first term of LHS, we obtain

$$(3.16) \quad \int_{\mathbb{R}} \partial_x \Phi \cdot \partial_x w \circ \Phi \cdot \alpha \left(\frac{\partial_x (u \partial_x u + \partial_t u) \circ \Phi}{\partial_x \Phi(x)} \right) + w \circ \Phi \cdot (u \partial_x u + \partial_t u) \circ \Phi \, dx$$

$$(3.17) \quad = - \int_{\mathbb{R}} \partial_x \Phi \cdot \partial_x w \circ \Phi \cdot 2\alpha \left(\frac{(\partial_x u)^2 \circ \Phi}{\partial_x \Phi(x)} \right) \, dx$$

$$(3.18) \quad \Rightarrow \int_{\mathbb{R}} \partial_x w \circ \Phi \cdot \alpha \left(\frac{\partial_x (u \partial_x u + \partial_t u) \circ \Phi}{1} \right) + w \circ \Phi \cdot (u \partial_x u + \partial_t u) \circ \Phi \, dx$$

$$(3.19) \quad = \int_{\mathbb{R}} \partial_x w \circ \Phi \cdot 2\alpha \left(\frac{(\partial_x u)^2 \circ \Phi}{1} \right) \, dx.$$

Applying a change of variable to (3.18), we obtain

$$(3.20) \quad \int_{\mathbb{R}} \partial_x w \cdot \alpha \left[\frac{\partial_x (u \partial_x u + \partial_t u)}{\partial_x \Phi \circ \Phi^{-1}} \right] + w \cdot \frac{(u \partial_x u + \partial_t u)}{\partial_x \Phi \circ \Phi^{-1}} \, dx$$

$$(3.21) \quad = \int_{\mathbb{R}} \partial_x w \cdot 2\alpha \left(\frac{(\partial_x u)^2}{\partial_x \Phi \circ \Phi^{-1}} \right) \, dx$$

$$(3.22) \quad \Rightarrow -\alpha \partial_x \left(\frac{\partial_x (u \partial_x u + \partial_t u)}{\partial_x \Phi \circ \Phi^{-1}} \right) + \frac{(u \partial_x u + \partial_t u)}{\partial_x \Phi \circ \Phi^{-1}} = -2\alpha \partial_x \left(\frac{(\partial_x u)^2}{\partial_x \Phi \circ \Phi^{-1}} \right)$$

We keep track of the derivatives of $\partial_x \Phi$ as Eulerian density ρ , defined by

$$(3.23) \quad \rho(\Phi(x)) := \frac{1}{\partial_x \Phi(x)},$$

resulting in the equation

$$(3.24) \quad -\alpha \partial_x (\rho \partial_x (u \partial_x u + \partial_t u)) + \rho (u \partial_x u + \partial_t u) = -2\alpha \partial_x (\rho (\partial_x u)^2).$$

Define the operator

$$(3.25) \quad \mathcal{H}_v : u \mapsto vu - \alpha \partial_x (v \partial_x u).$$

Then, equation (3.24) can be re-written as

$$(3.26) \quad \partial_t u + u \partial_x u = -\mathcal{H}_\rho^{-1} \left(\partial_x \left(2\alpha \rho [\partial_x u]^2 \right) \right).$$

By differentiating the map $t \mapsto \rho(t, F(t, x))$ and applying the chain rule, we obtain

$$(3.27) \quad \partial_t \rho + \partial_x \rho u = -\frac{\partial_x \dot{\Phi}(X)}{(\partial_x \Phi(x))^2} = -\rho \partial_x u, \Rightarrow \partial_t \rho = -(\partial_x \rho)u - (\partial_x u)\rho.$$

This yields the momentum form of the modified Burgers' equation,

$$(3.28) \quad \begin{cases} \partial_t(\rho u) + \partial_x(\rho u^2) = -2\alpha \cdot \rho \cdot \mathcal{H}_\rho^{-1} \left(\partial_x \left(\rho [\partial_x u]^2 \right) \right) \\ \partial_t \rho + \partial_x(\rho u) = 0. \end{cases}$$

We can recast the above equation into the conservative form of the Burgers' equation by using the identity $(\mathcal{A}\mathcal{B})^{-1} = \mathcal{B}^{-1}\mathcal{A}^{-1}$ for linear operators \mathcal{A} and \mathcal{B} to obtain

$$(3.29) \quad \partial_x^{-1} \left(\rho \mathcal{H}_\rho^{-1} \left(\partial_x \left(\rho [\partial_x u]^2 \right) \right) \right)$$

$$(3.30) \quad \partial_x^{-1} \left(([\rho - \alpha \partial_x \rho \partial_x] \rho^{-1})^{-1} \left(\partial_x \left(\rho [\partial_x u]^2 \right) \right) \right)$$

$$(3.31) \quad = \left((1 - \alpha \partial_x \rho \partial_x \rho^{-1}) \partial_x \right)^{-1} \partial_x \left(\rho [\partial_x u]^2 \right)$$

$$(3.32) \quad = (\partial_x - \alpha \partial_x \rho \partial_x \rho^{-1} \partial_x)^{-1} \partial_x \left(\rho [\partial_x u]^2 \right)$$

$$(3.33) \quad = (1 - \alpha \rho \partial_x \rho^{-1} \partial_x)^{-1} \left(\rho [\partial_x u]^2 \right)$$

$$(3.34) \quad = (\rho^{-1} - \alpha \partial_x \rho^{-1} \partial_x)^{-1} \left([\partial_x u]^2 \right)$$

$$(3.35) \quad = \mathcal{H}_{\rho^{-1}}^{-1} \left([\partial_x u]^2 \right).$$

The resulting, conservative form of the modified Burgers' equation is given by

$$(3.36) \quad \partial_t(\rho u) + \partial_x \left(\rho u^2 + 2\alpha \mathcal{H}_{\rho^{-1}}^{-1} \left((\partial_x u)^2 \right) \right) = 0.$$

Adding the pressure $P(\rho)$ yields the modified unidimensional Euler equation

$$(3.37) \quad \partial_t(\rho u) + \partial_x \left(\rho u^2 + P(\rho) + 2\alpha \mathcal{H}_{\rho^{-1}}^{-1} \left((\partial_x u)^2 \right) \right) = 0.$$

3.4. The multidimensional case using the log determinantal barrier.

We propose using the log determinant potential on \mathcal{E} , resulting in

$$(3.38) \quad \psi(\Phi, \Phi') = \frac{1}{2} \int_{\mathcal{M}} \|\Phi(x)\|^2 dx + \alpha \int_{\mathcal{M}} -\log \det(\Phi'(x)) dx.$$

Applied to symmetric and positive matrices, the log determinantal potential coincides with the entropy of a centered Gaussian and the self-concordant barrier function of semidefinite programming [46]. Applied to the Jacobian of the deformation Φ in x , it measures the volume of positional uncertainty of a particle initially at x .

3.5. Multidimensional case, Lagrangian description.

The derivative is

$$(3.39) \quad [\mathbb{D}\psi(\Phi, \Phi')](U, U') = \int_{\mathcal{M}} \langle U(x), \Phi(x) \rangle dx + \alpha \int_{\mathcal{M}} -\text{tr} \left(U'(x) [\Phi'(x)]^{-1} \right) dx.$$

The resulting gradient map with respect to the L^2 inner product is given as

$$(3.40) \quad \nabla\psi(\Phi, \Phi') = \left(\Phi, -\alpha [\Phi'(x)]^{-T} \right).$$

The second derivative map is given by

$$(3.41) \quad [D^2\psi(\Phi, \Phi')]((U, U'), (V, V'))$$

$$(3.42) \quad = \int_{\mathcal{M}} \langle U(x), V(x) \rangle dx + \alpha \int_{\mathcal{M}} \text{tr} \left(V'(x) [\Phi'(x)]^{-1} U'(x) [\Phi'(x)]^{-1} \right) dx.$$

We note that while ψ is not convex on \mathcal{E} , it is convex on convex subsets of \mathcal{M} . Using the L^2 inner product, we can interpret its Hessian as an operator from \mathcal{E} to \mathcal{E} ,

$$(3.43) \quad [D^2\psi(\Phi, \Phi')]((U, U')) = \left(U, \alpha \left([\Phi']^{-1} U' [\Phi']^{-1} \right)^T \right).$$

Under the same assumptions as above, we compute the third derivative operator as

$$(3.44) \quad [D^3\psi(\Phi, \Phi')]((U, U'), (V, V'), (W, W'))$$

$$(3.45) \quad = -\alpha \int_{\mathcal{M}} \text{tr} \left(V'(x) [\Phi'(x)]^{-1} U'(x) [\Phi'(x)]^{-1} W'(x) [\Phi'(x)]^{-1} \right) dx$$

$$(3.46) \quad -\alpha \int_{\mathcal{M}} \text{tr} \left(V'(x) [\Phi'(x)]^{-1} W'(x) [\Phi'(x)]^{-1} U'(x) [\Phi'(x)]^{-1} \right) dx$$

and interpret it as a map from $\mathcal{E} \otimes \mathcal{E}$ to \mathcal{E} ,

$$(3.47) \quad [D^3\psi(\Phi, \Phi')]((U, U'), (V, V'))$$

$$(3.48) \quad = \left(0, -\alpha \left([\Phi']^{-1} V' [\Phi']^{-1} U' [\Phi']^{-1} + [\Phi']^{-1} U' [\Phi']^{-1} V' [\Phi']^{-1} \right)^T \right).$$

As in the unidimensional case, we compute the parallel transport as

$$(3.49) \quad [\nabla_{V, V'}(\Phi, \Phi')](U, U') = \left(0, \partial V [\partial\Phi]^{-1} \partial U + \partial U [\partial\Phi]^{-1} \partial V \right).$$

Defining $S := V' [\Phi']^{-1} U' + U' [\Phi']^{-1} V'$, we can now obtain the projected parallel transport through the variational formulation

$$(3.50) \quad [\nabla_V(\Phi)](U) = \arg \min_{W \in T_{\Phi} \mathcal{A}} \int_{\mathcal{M}} \|W\|^2 dx + \alpha \int_{\mathcal{M}} \text{tr} \left((DW - S) [D\Phi]^{-1} (DW - S) [D\Phi]^{-1} \right) dx,$$

where every term in the integrands implicitly depends on x . In the computation below, we use the standard inner product for matrices $\langle A, B \rangle := \text{tr}(AB^T)$. By taking an arbitrary variation $\delta W \in T_{\Phi} \mathcal{M} = H^1(\mathbb{R}^d)$, we obtain

$$\begin{aligned} \forall \delta W &: \int \langle \delta W, W \rangle + \alpha \text{tr} \left((D\delta W) [D\Phi]^{-1} (DW - S) [D\Phi]^{-1} \right) dx = 0 \\ \Leftrightarrow \forall \delta W &: \int \langle \delta W, W \rangle + \alpha \langle D\delta W, [D\Phi]^{-1} (DW - S) [D\Phi]^{-1} \rangle dx = 0 \\ \Leftrightarrow \forall \delta W &: \int \langle \delta W, W \rangle - \alpha \langle \delta W, \text{div} \left([D\Phi]^{-1} (DW - S) [D\Phi]^{-1} \right) \rangle dx = 0 \\ \Leftrightarrow W &- \alpha \text{div} \left([D\Phi]^{-1} DW [D\Phi]^{-1} \right) = -\alpha \text{div} \left([D\Phi]^{-1} S [D\Phi]^{-1} \right). \end{aligned}$$

As a result of the above, dual parallel transport on \mathcal{M} satisfies

$$(3.51) \quad [\nabla_{\mathbf{V}}(\Phi)](U) = \hat{\mathcal{H}}_{\Phi}^{-1} \left(-\alpha \operatorname{div} \left([\mathbf{D}\Phi]^{-1} (\mathbf{D}\mathbf{V}[\mathbf{D}\Phi]^{-1} \mathbf{D}U + \mathbf{D}U[\mathbf{D}\Phi]^{-1} \mathbf{D}\mathbf{V}) [\mathbf{D}\Phi]^{-1} \right) \right)$$

with $\hat{\mathcal{H}}_{\Phi} W := W - \alpha \operatorname{div} ([\mathbf{D}\Phi]^{-1} \mathbf{D}W[\mathbf{D}\Phi]^{-1})$. The resulting geodesic equations are

$$(3.52) \quad \ddot{\Phi} = \mathcal{H}[\Phi]^{-1} \left(-2\alpha \operatorname{div} \left([\mathbf{D}\Phi]^{-1} \mathbf{D}\dot{\Phi}[\mathbf{D}\Phi]^{-1} \mathbf{D}\dot{\Phi}[\mathbf{D}\Phi]^{-1} \right) \right).$$

3.6. Multidimensional case, Eulerian description. As in the unidimensional case, we write \mathbf{u} as

$$(3.53) \quad \dot{\Phi}(x) =: \mathbf{u}(\Phi(x)) \quad \Rightarrow \quad \ddot{\Phi}(x) = [\mathbf{D}\mathbf{u}(\Phi(x))] \mathbf{u}(\Phi(x)) + \partial_t \mathbf{u}(\Phi(x))$$

and ρ as

$$(3.54) \quad \rho(\Phi(x)) = \frac{1}{\det(\mathbf{D}\Phi(x))}.$$

Plugging this into the geodesic equation

$$(3.55) \quad -\alpha \operatorname{div} \left([\mathbf{D}\Phi]^{-1} \mathbf{D}\ddot{\Phi}[\mathbf{D}\Phi]^{-1} \right) + \ddot{\Phi} = -2\alpha \operatorname{div} \left([\mathbf{D}\Phi]^{-1} \mathbf{D}\dot{\Phi}[\mathbf{D}\Phi]^{-1} \mathbf{D}\dot{\Phi}[\mathbf{D}\Phi]^{-1} \right),$$

we obtain as before

$$(3.56) \quad -\alpha \operatorname{div} \left([\mathbf{D}\Phi]^{-1} \mathbf{D}\ddot{\Phi}[\mathbf{D}\Phi]^{-1} \right) + \ddot{\Phi} = -2\alpha \operatorname{div} \left([\mathbf{D}\Phi]^{-1} [\mathbf{D}\mathbf{u}] \circ \Phi [\mathbf{D}\mathbf{u}] \circ \Phi \right).$$

By multiplying with a test function $x \mapsto \mathbf{w}(\Phi(x))$ and integrating, we obtain

$$(3.57) \quad -\alpha \int \langle \mathbf{w} \circ \Phi, \operatorname{div} \left([\mathbf{D}\Phi]^{-1} \mathbf{D}\ddot{\Phi}[\mathbf{D}\Phi]^{-1} \right) \rangle dx + \int \langle \mathbf{w} \circ \Phi, \ddot{\Phi} \rangle dx$$

$$(3.58) \quad = -2\alpha \int \langle \mathbf{w} \circ \Phi, \operatorname{div} \left([\mathbf{D}\Phi]^{-1} [\mathbf{D}\mathbf{u}] \circ \Phi [\mathbf{D}\mathbf{u}] \circ \Phi \right) \rangle dx.$$

We now apply integration by parts and plug in the definition of $\ddot{\Phi}$ to obtain

$$(3.59) \quad \alpha \int \operatorname{tr} \left(\mathbf{D}\mathbf{w} \mathbf{D}([\mathbf{D}\mathbf{u}]\mathbf{u} + \partial_t \mathbf{u}) \right) (\Phi(x)) dx - \int \langle \mathbf{w}, [\mathbf{D}\mathbf{u}]\mathbf{u} + \partial_t \mathbf{u} \rangle (\Phi(x)) dx$$

$$(3.60) \quad = 2\alpha \int \operatorname{tr} \left(\mathbf{D}\mathbf{w} [\mathbf{D}\mathbf{u}] [\mathbf{D}\mathbf{u}] \right) (\Phi(x)) dx.$$

Changing variables $x \mapsto \Phi(x)$, we obtain

$$(3.61) \quad \alpha \int \rho \operatorname{tr} \left(\mathbf{D}\mathbf{w} \mathbf{D}([\mathbf{D}\mathbf{u}]\mathbf{u} + \partial_t \mathbf{u}) \right) dx + \int \rho \langle \mathbf{w}, [\mathbf{D}\mathbf{u}]\mathbf{u} + \partial_t \mathbf{u} \rangle dx$$

$$(3.62) \quad = 2\alpha \int \rho \operatorname{tr} \left(\mathbf{D}\mathbf{w} [\mathbf{D}\mathbf{u}] [\mathbf{D}\mathbf{u}] \right) dx.$$

We again apply integration by parts, together with the fundamental lemma of the calculus of variations to obtain

$$(3.63) \quad -\alpha \operatorname{div} (\rho \mathbf{D}([\mathbf{D}\mathbf{u}]\mathbf{u} + \partial_t \mathbf{u})) + \rho([\mathbf{D}\mathbf{u}]\mathbf{u} + \partial_t \mathbf{u}) = -2\alpha \operatorname{div} (\rho [\mathbf{D}\mathbf{u}] [\mathbf{D}\mathbf{u}]).$$

As before, the equation for the conservation of mass is

$$(3.64) \quad \partial_t \rho = -\operatorname{div}(\rho \mathbf{u}) \Rightarrow \partial_t (\rho \mathbf{u}) = (\partial_t \mathbf{u}) \rho - \mathbf{u} \operatorname{div}(\rho \mathbf{u}) = (\partial_t \mathbf{u}) \rho - \mathbf{u} [\operatorname{D}\rho] \mathbf{u} - \rho \operatorname{div} \mathbf{u}.$$

We can now recast the equation as

$$(3.65) \quad \partial_t \mathbf{u} + [\operatorname{D}\mathbf{u}] \mathbf{u} + 2\alpha (\rho - \alpha \operatorname{div} \rho \operatorname{D})^{-1} \operatorname{div}(\rho [\operatorname{D}\mathbf{u}] [\operatorname{D}\mathbf{u}]) = 0.$$

In order to derive a momentum conservation law, we multiply with ρ and use the equation for mass conservation,

$$(3.66) \quad \partial_t (\rho \mathbf{u}) + \mathbf{u} [\operatorname{D}\rho] \mathbf{u} + \rho \operatorname{div} \mathbf{u} + \rho [\operatorname{D}\mathbf{u}] \mathbf{u} + 2\alpha \rho (\rho - \alpha \operatorname{div} \rho \operatorname{D})^{-1} \operatorname{div}(\rho [\operatorname{D}\mathbf{u}] [\operatorname{D}\mathbf{u}]) = 0.$$

We now use the identity

$$\begin{aligned} \operatorname{div}(\rho \mathbf{u} \otimes \mathbf{u}) &= \operatorname{div}(\rho \mathbf{u}) \mathbf{u} + \rho \operatorname{div}(\mathbf{u}) \\ &= \langle \nabla \rho, \mathbf{u} \rangle \mathbf{u} + (\rho \operatorname{div} \mathbf{u}) \mathbf{u} + \rho \operatorname{div} \mathbf{u} \\ &= \mathbf{u} [\operatorname{D}\rho] \mathbf{u} + \rho [\operatorname{D}\mathbf{u}] \mathbf{u} + \rho \operatorname{div} \mathbf{u}. \end{aligned}$$

to conclude

$$(3.67) \quad \partial_t (\rho \mathbf{u}) + \operatorname{div}(\rho \mathbf{u} \otimes \mathbf{u}) + 2\alpha \rho (\rho - \alpha \operatorname{div} \rho \operatorname{D})^{-1} \operatorname{div}(\rho [\operatorname{D}\mathbf{u}] [\operatorname{D}\mathbf{u}]) = 0.$$

We now use the identity $(\mathcal{A}\mathcal{B})^{-1} = \mathcal{B}^{-1}\mathcal{A}^{-1}$ for linear operators \mathcal{A} and \mathcal{B} to obtain

$$(3.68) \quad \partial_t (\rho \mathbf{u}) + \operatorname{div}(\rho \mathbf{u} \otimes \mathbf{u}) + 2\alpha \rho (\rho - \alpha \operatorname{div} \rho \operatorname{D})^{-1} \operatorname{div}(\rho [\operatorname{D}\mathbf{u}] [\operatorname{D}\mathbf{u}]) = 0$$

$$(3.69) \quad \Leftrightarrow \partial_t (\rho \mathbf{u}) + \operatorname{div}(\rho \mathbf{u} \otimes \mathbf{u}) + 2\alpha (\operatorname{Id} - \alpha \operatorname{div} \rho \operatorname{D} \rho^{-1})^{-1} \operatorname{div}(\rho [\operatorname{D}\mathbf{u}] [\operatorname{D}\mathbf{u}]) = 0$$

$$(3.70) \quad \Leftrightarrow \partial_t (\rho \mathbf{u}) + \operatorname{div}(\rho \mathbf{u} \otimes \mathbf{u}) + 2\alpha (\operatorname{div}^{-1} - \alpha \rho \operatorname{D} \rho^{-1})^{-1} \rho [\operatorname{D}\mathbf{u}] [\operatorname{D}\mathbf{u}] = 0$$

$$(3.71) \quad \Leftrightarrow \partial_t (\rho \mathbf{u}) + \operatorname{div}(\rho \mathbf{u} \otimes \mathbf{u}) + 2\alpha \operatorname{div} \left((\operatorname{Id} - \alpha \rho \operatorname{D} \rho^{-1} \operatorname{div})^{-1} \rho [\operatorname{D}\mathbf{u}] [\operatorname{D}\mathbf{u}] \right) = 0$$

$$(3.72) \quad \Leftrightarrow \partial_t (\rho \mathbf{u}) + \operatorname{div}(\rho \mathbf{u} \otimes \mathbf{u}) + 2\alpha \operatorname{div} \left((\rho^{-1} - \alpha \operatorname{D} \rho^{-1} \operatorname{div})^{-1} [\operatorname{D}\mathbf{u}] [\operatorname{D}\mathbf{u}] \right) = 0.$$

Writing $\mathcal{H}_v: \mathbf{u} \mapsto v\mathbf{u} - \alpha \operatorname{D}(v \operatorname{div} \mathbf{u})$ we obtain

$$(3.73) \quad \begin{cases} \partial_t (\rho \mathbf{u}) + \operatorname{div} \left(\rho \mathbf{u}^2 + P(\rho) + 2\alpha \mathcal{H}_{\rho^{-1}}^{-1}([\operatorname{D}\mathbf{u}][\operatorname{D}\mathbf{u}]) \right) = 0 \\ \partial_t \rho + \partial_x(\rho \mathbf{u}) = 0. \end{cases}$$

4. Numerical experiments.

4.1. Overview. The numerical experiments in this section serve the dual purpose of illustrating the behavior of solutions to the modified equations and providing proof of the concept of using the latter for numerical purposes. Classical methods such as the Lax-Friedrichs and Lax-Wendroff methods take the flux of the PDE as input. They therefore apply directly to the regularized equation in the form of (3.73). We emphasize that the results in this section are not yet meant to be fair comparisons to the state-of-the-art in simulating compressible flows. Such a comparison requires comparing to stronger baselines (such as (W)ENO schemes) and introducing an efficient approximation for the inverse of $\mathcal{H}_{\rho^{-1}}^{-1}$. This will be the subject of future work.

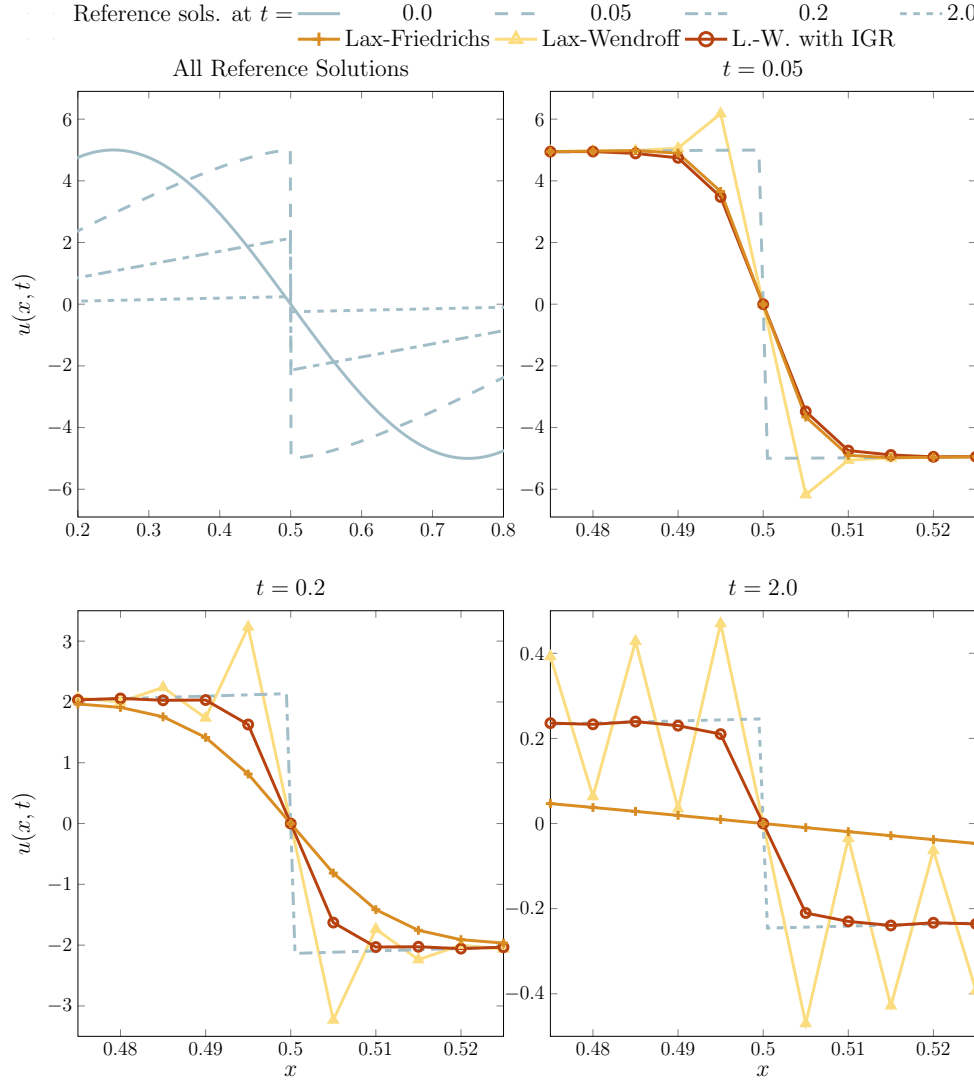


FIG. 6. **Results on the unidimensional Burgers Equation:** We solve Burgers' equation with initial conditions $u(x, 0) = 5 \sin(2\pi x)$ and periodic boundary conditions. The solution at $t \in \{0.05, 0.2, 2.0\}$ features a shock of decreasing magnitude. We compare Lax-Friedrichs and Lax-Wendroff methods [41] on the unregularized Burgers equation to Lax-Wendroff with geometric regularization. Lax-Friedrichs smears out shocks and (unregularized) Lax-Wendroff develops spurious oscillations. Information geometric regularization (IGR) avoids these effects.

4.2. Application to Burger's equation. We begin by investigating the behavior of the regularized unidimensional Burgers equation. We use sinusoidal initial conditions and construct a reference solution using characteristics. We use the Lax-Friedrichs and Lax-Wendroff methods [41] to solve the unregularized (2.3). To solve the regularized Burgers equation (1.2), we use the Lax-Wendroff method on the momentum equation and the Lax-Friedrichs method on the density component. Lax-Friedrichs results in excessive smoothness and Lax-Wendroff leads to oscillations.

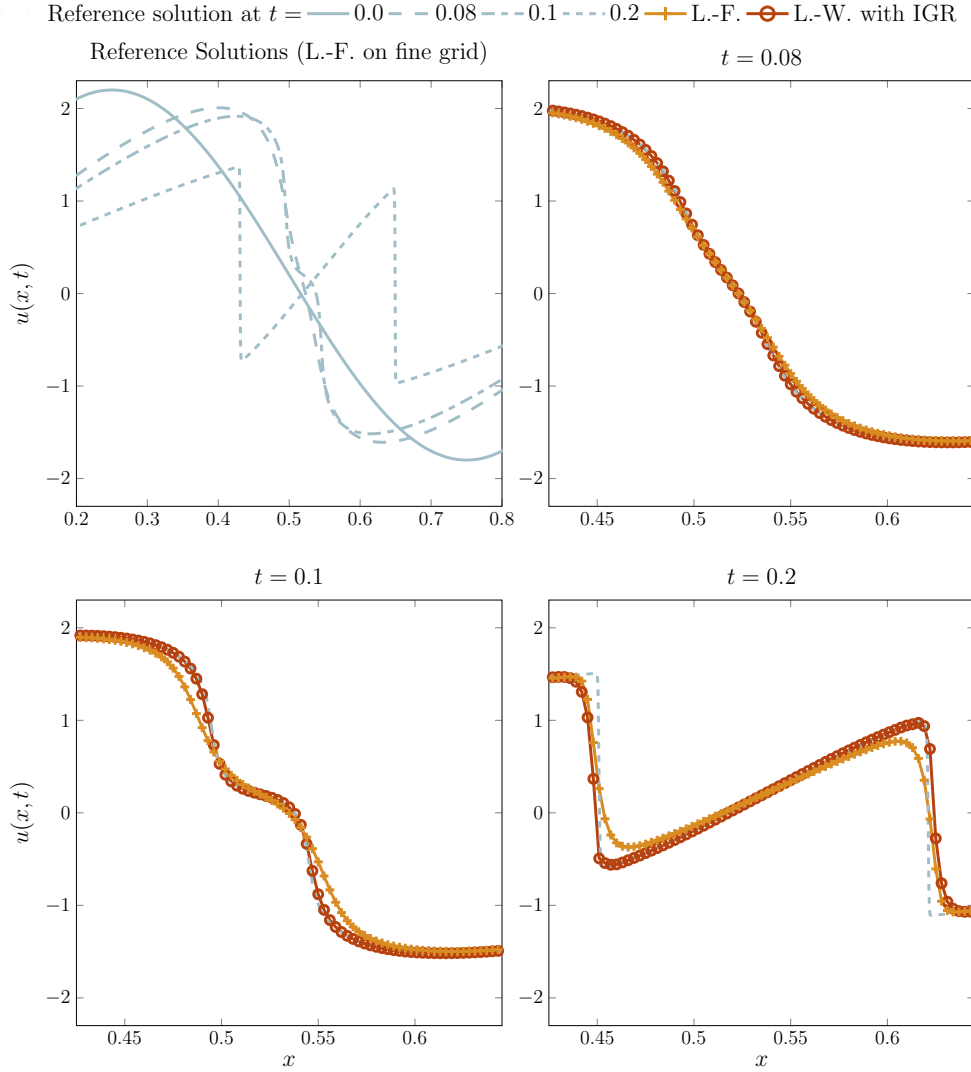


FIG. 7. **Results on the unidimensional Euler Equation:** We apply information geometric regularization (IGR) solved with the Lax-Wendroff method to the unidimensional Euler equation, comparing it to a Lax-Friedrichs solution on the same resolution and a high-accuracy reference solution. IGR produces a nonsingular solution without the excessive smoothing of Lax-Friedrichs.

4.2.1. Effect of Mach number.

4.3. Application to unidimensional Euler equation. We now investigate the application of information geometric regularization to the unidimensional Euler equation. Throughout this section, the pressure is given by $P(\rho) = a\rho^\gamma$.

4.3.1. Comparison to unregularized Lax-Friedrichs. As a first step, we repeat the experiment of Figure 6 with the unidimensional Euler equation. We use the Lax-Wendroff method for solving the regularized equation (1.2) to emphasize it

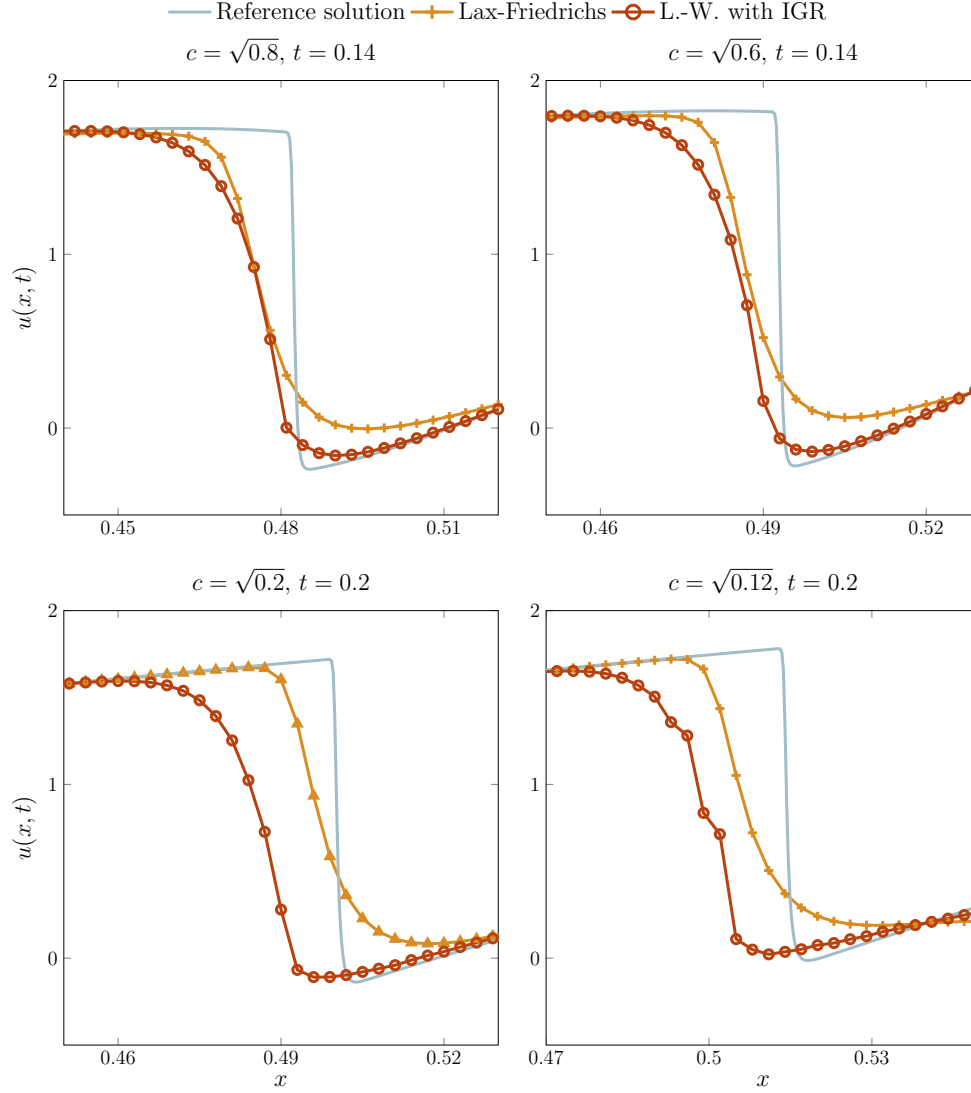


FIG. 8. **Varying sound speeds.** We repeat the experiment of Figure 7 for a range of different sound speeds to illustrate the robustness of our approach (note the zoom in the x -axis).

not requiring numerical viscosity. Applied to the unregularized Euler equation, this scheme produces singular solutions, emphasizing the importance of our modification. In Figure 7, we compare this approach to a Lax-Friedrichs solution with the same mesh size and a reference solution obtained from Lax-Friedrichs with a very fine mesh. We observe that due to the viscosity, the Lax-Friedrichs solution underestimates the magnitude of the shock, in contrast to Lax-Wendroff with IGR.

We next investigate the effects of varying sound speed, and thus, Mach number. To this end, we rerun the experiments with $a = \{0.8, 0.6, 0.2, 0.12\}$, resulting in sound speed $c = \sqrt{a}$. We observe that the approximation quality is mostly preserved, with a slight loss of smoothness for large Mach number ≈ 11 .

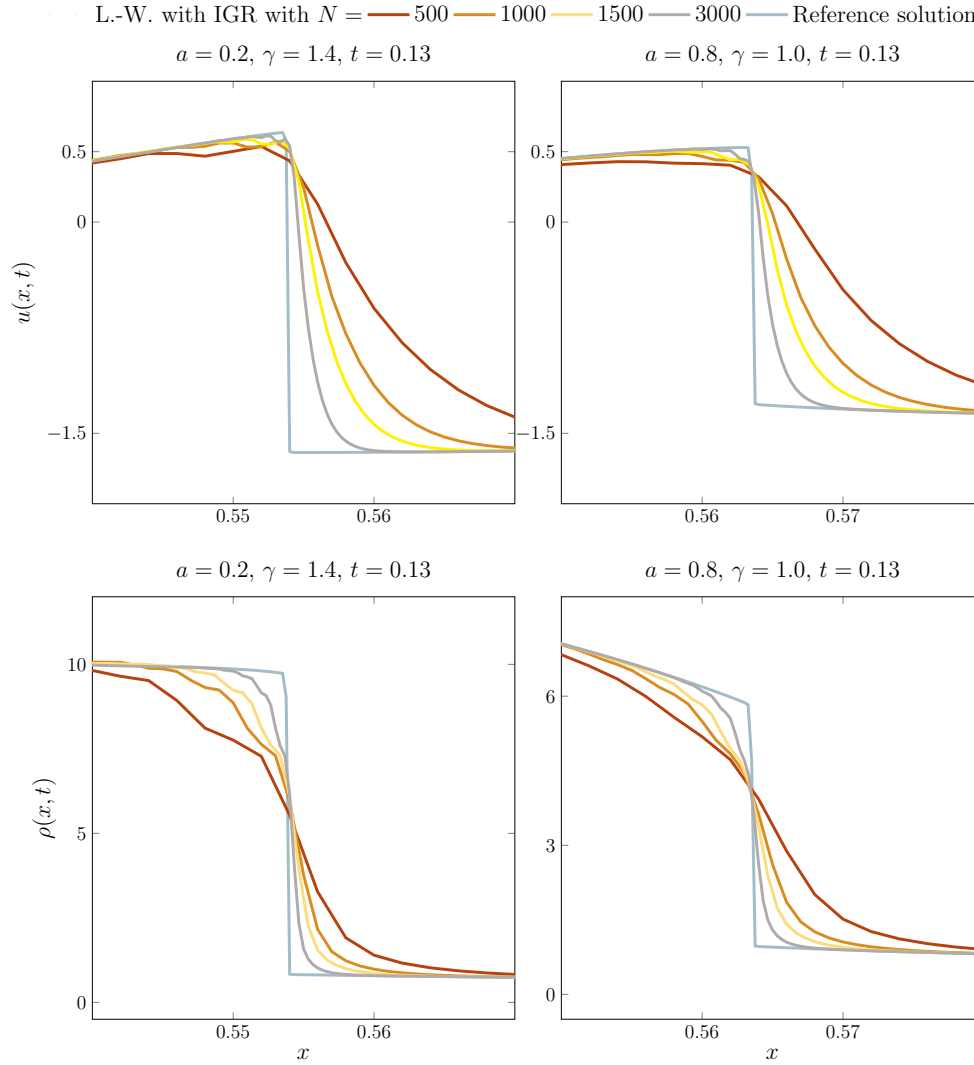


FIG. 9. **Grid refinement.** As we increase the grid size N and decrease $\alpha \propto N^{-2}$, the regularized solution converges to the reference solution.

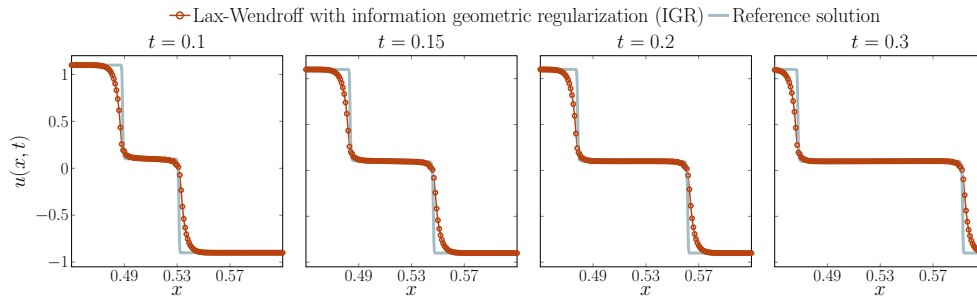


FIG. 10. **Shock speed.** IGR appears to preserve the speed of shock propagation exactly.

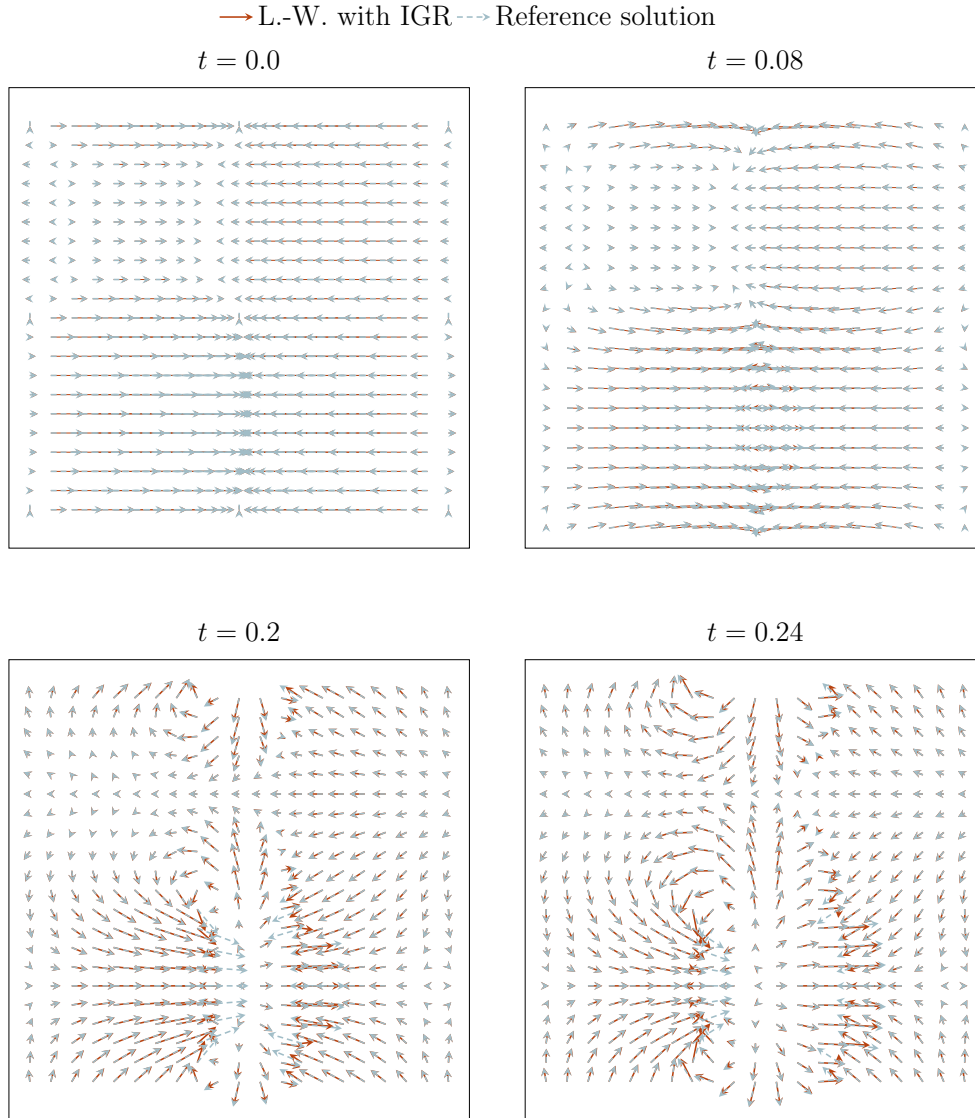


FIG. 11. *Two-dimensional Euler equation:* We compare Lax-Wendroff with information geometric regularization with 500^2 grid points to a reference solution computed by Lax Friedrichs with 2000^2 grid points. Up to a few points near the shock front, the two solutions are in agreement.

4.3.2. Grid refinement and vanishing regularization. A key question for the practical applicability of information geometric regularization is whether the numerical approximation of the regularized equation approximates the entropy solution as the mesh width h and α tend to zero. The scaling $h^2 \approx \alpha \rightarrow 0$ is especially appealing as it maintains a bounded condition number of the discretized $\mathcal{H}_{\rho-1}$, enabling its efficient inversion. As shown in Figure 9, this scaling systematically improves the approximation properties. This serves as preliminary evidence of the practical utility of the proposed regularization.

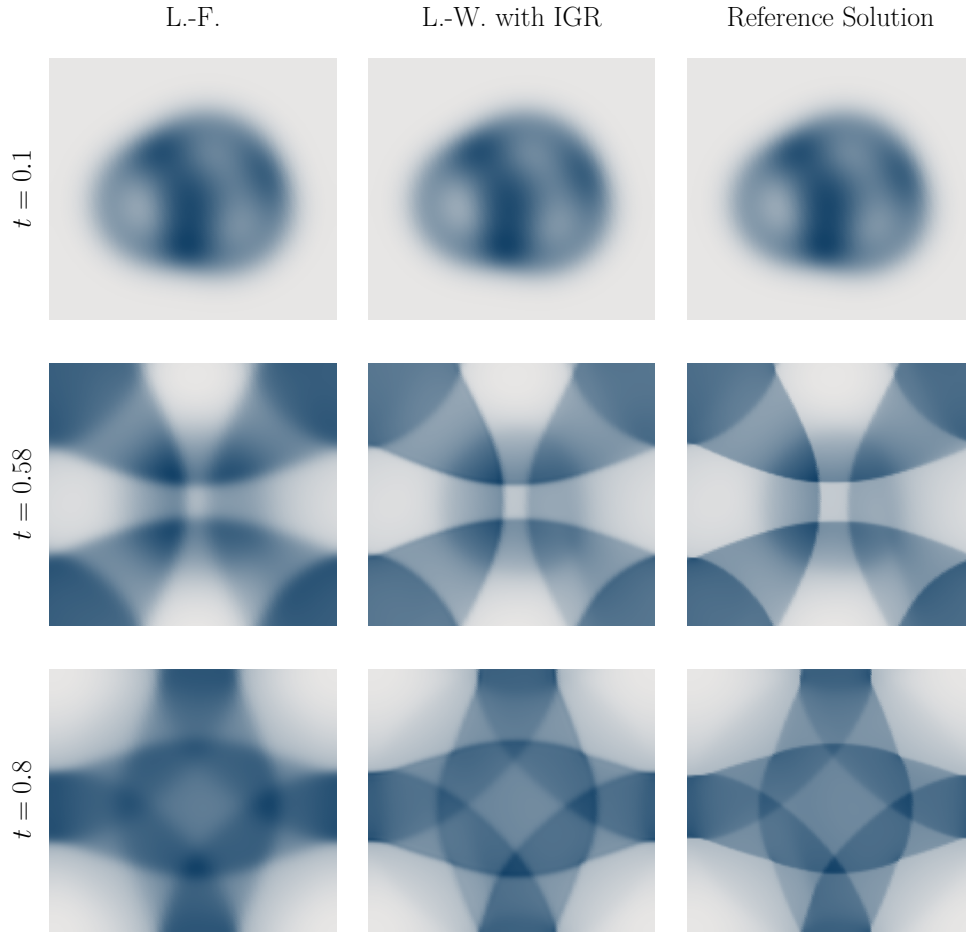


FIG. 12. We compare the density obtained by Lax-Friedrichs and Lax-Wendroff with IGR on 500^2 grid points to a reference solution computed by Lax-Friedrichs with 4000^2 grid points.

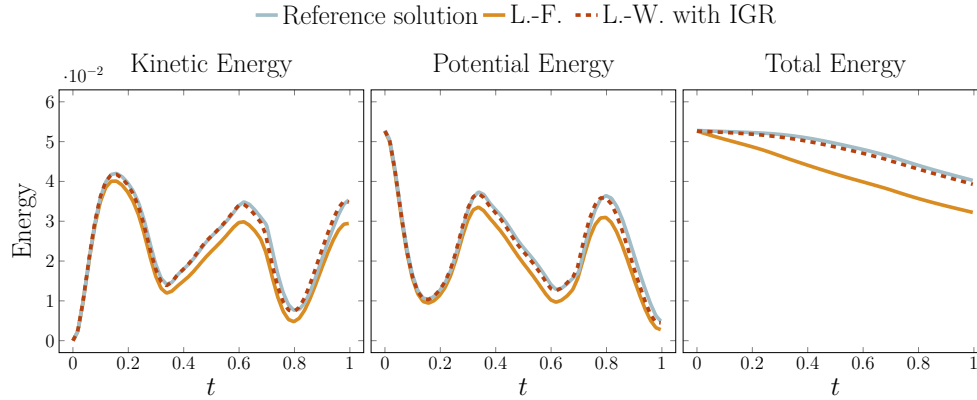


FIG. 13. We compare the energy dissipation of Lax-Friedrichs and Lax-Wendroff with IGR on 500^2 grid points to that of a reference solution computed by Lax-Friedrichs with 4000^2 grid points.

4.3.3. Shock speed. A key shortcoming of the prior work of [10] was that near-shocks in the regularized system do not propagate with the correct velocity [10, Figure 2]. In contrast to their work, and similar to that of [31], the regularization proposed in this work can be written in momentum-conservation form (1.2). We believe that this feature explains our empirical observation that the information geometric regularization maintains the correct shock speed, as illustrated in Figure 10.

4.4. Application to multidimensional Euler equation. Finally, we provide numerical results on two-dimensional information geometric regularization of the Euler equation. We use Lax-Wendroff with information geometric regularization (IGR) and compare with results obtained by Lax-Friedrichs on a high-resolution grid.

4.4.1. Velocity Profile. We begin by showing the velocity profiles for initial conditions given by laminar sine waves. As shown in Figure 11, the IGR solution agrees with the reference solution, except for some points near the shock front.

4.4.2. Density and Energy Dissipation. Furthermore, we provide a comparison of density and energy dissipation solutions obtained by Lax-Friedrichs on a low-resolution grid, Lax-Wendroff with information geometric regularization on the same low-resolution grid, and Lax-Friedrichs on a high-resolution grid. For this numerical experiment, we choose the triple blast wave initial condition

$$\mathbf{u}(\mathbf{x}, 0) = \mathbf{0}, \rho(\mathbf{x}, 0) = \frac{\beta}{3\sigma} e^{-\frac{\|\mathbf{x}-\mathbf{c}_1\|^2}{2\sigma^2}} + \frac{\beta}{3\sigma} e^{-\frac{\|\mathbf{x}-\mathbf{c}_2\|^2}{2\sigma^2}} + \frac{\beta}{3\sigma} e^{-\frac{\|\mathbf{x}-\mathbf{c}_3\|^2}{2\sigma^2}} + C_0,$$

where $\beta = 0.25$, $\sigma = 0.08$, $C_0 = 1.0$, $\mathbf{c}_1 = (0.4, 0.45)$, $\mathbf{c}_2 = (0.55, 0.55)$, $\mathbf{c}_3 = (0.6, 0.42)$. As shown in Figure 13, the numerical solution obtained with information geometric regularization prevents systematic loss of energy.

5. Comparison, conclusion, and outlook.

5.1. Comparison to related work. The earliest work proposing inviscid regularization in a spirit similar to ours is a series of papers by Bhat and Fetecau [12, 11, 10], motivated by ideas of Leray [40]. In the case of Burgers' equation, their regularization amounts to setting $\rho \equiv 1$ in (3.36) and shows promising results. However, its generalization to the Euler equation fails to maintain the shock speed of the nominal equation, greatly limiting its usefulness for numerical purposes. Recently, [31] proposed a family of inviscid and nondispersive regularizations for the unidimensional Euler equation, based on a similar regularization for the shallow water equation [22]. The members of this family can be written in conservation form and thus maintain the correct shock speed. They are parametrized by a function $\mathcal{A} : \mathbb{R} \rightarrow \mathbb{R}$ of the density. In the special case of vanishing pressure and $\mathcal{A}(\rho) := \rho$, this regularization coincides with (3.36). While [31] does not give this case special consideration and their proposed regularization is limited to the unidimensional case, their theoretical results may aid in understanding information geometric regularization. Numerous existing works apply viscous regularization adaptively, based on shock indicators [56, 50, 23, 27, 45, 8, 32, 15, 24, 9, 36]. A prototypical form of this ‘‘localized artificial diffusivity’’ (LAD) amounts to removing the elliptic operator and using the negative semidefinite part of $[\mathbf{D}\mathbf{u}]$ in information geometric regularization (IGR) (1.2)

$$(5.1) \quad \begin{cases} \partial_t \begin{pmatrix} \rho \mathbf{u} \\ \rho \end{pmatrix} + \operatorname{div} \begin{pmatrix} \rho \mathbf{u} \otimes \mathbf{u} + P(\rho) \mathbf{I} + \mathbf{F} \\ \rho \mathbf{u} \end{pmatrix} = \begin{pmatrix} \mathbf{f} \\ 0 \end{pmatrix} \\ \rho^{-1} \mathbf{F} - \alpha \mathbf{D}(\rho^{-1} \operatorname{div} \mathbf{F}) = 2\alpha [[\mathbf{D}\mathbf{u}]]_{\text{n.s.d}} [\mathbf{D}\mathbf{u}]. \end{cases}$$

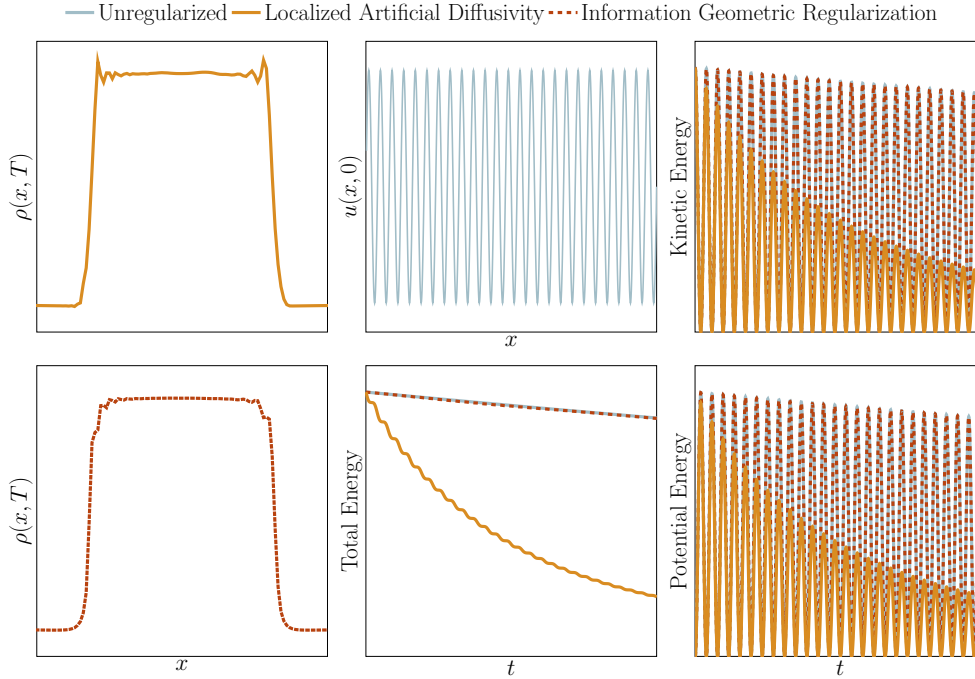


FIG. 14. **IGR and LAD.** Nonlocal information geometric regularization reduces oscillations of dispersive schemes at shocks (first column). In high-frequency waves, artificial diffusivity’s dissipative bias causes systematic loss of energy, as each downward slope of u looks like it could be a shock. Sign-indefinite information geometric regularization solves this problem (second, third column).

The regularization term \mathbf{F} of (1.2) mimics a nonlocal, nonsymmetric, and sign-indefinite diffusion. As shown in Figure 14, the nonlocality due to the elliptic problem in IGR reduces spurious oscillations in dispersive numerical schemes for a given parameter α . Where LAD can impose limits on the time step sizes due to the quadratic scaling of parabolic CFL numbers [36], our experiments suggest that increasing α in IGR imposes no such restrictions. A striking difference between IGR and LAD is that the IGR “diffusion tensor” is allowed to be nonsymmetric and sign-indefinite. As shown in Figure 14, this overcomes LAD’s systematic dissipative bias in high-frequency sound waves that otherwise requires specialized treatment [36]. The Riemannian geometry induced by the squared L^2 -distance in the original Euler equation is closely related to the Wasserstein geometry on the space of mass densities [14, 39] and the logdet regularization equals the negative Shannon entropy of the mass density. Information geometric regularization compromises between them. Similarly, [35, 3, 49, 42, 4, 17] combine optimal transport with entropic terms and information geometry and [37] use entropic regularization to solve explicitly inequality-constrained PDEs. In providing a geometric approach to modeling the energy dissipation in a shock our work is also related to the geometric treatment of thermodynamic systems in [28, 29, 30, 57].

5.2. Conclusion and outlook. In this work, we have proposed an information geometric regularization of the barotropic compressible Euler equation and provided a proof of concept for its numerical application. To the best of our knowledge, this is the first work that regularizes continuum mechanical equations by modifying the

geometry of the manifold of deformation maps. It thus opens up numerous directions for future work, including the application to other systems of PDEs, the use of different geometries, as well as the theoretical and numerical study of the resulting equations. For the sake of concreteness and conciseness, we have restricted this work to the case of the barotropic Euler equation and the information geometry induced by the log determinantal barrier function. However, generalizations to different geometries and related equations like the Navier Stokes and general Euler equations are straightforward to derive. An improved theoretical understanding of our approach will be crucial to identifying its most promising applications.

5.3. Toward information geometric mechanics. Our work combines the geometry governing the inertial movement of individual particles with the information geometry of distributions of particles. It thus takes the first step toward developing *information geometric mechanics* that accounts for the geometries not just of fundamental physical laws governing describing microscopic behavior, but also of the statistical summaries describing their emergent macroscopic behavior.

Acknowledgments. The authors gratefully acknowledge support from the Air Force Office of Scientific Research (award number FA9550-23-1-0668, Information Geometric Regularization for Simulation and Optimization of Supersonic Flow, PM Dr. Fariba Fahroo). RC acknowledges support through a PURA travel award from the Georgia Tech Office of Undergraduate Education.

REFERENCES

- [1] S.-I. AMARI, *Information geometry and its applications*, vol. 194, Springer, 2016.
- [2] S.-I. AMARI AND A. CICHOCKI, *Information geometry of divergence functions*, Bulletin of the polish academy of sciences. Technical sciences, 58 (2010), pp. 183–195.
- [3] S.-I. AMARI, R. KARAKIDA, AND M. OIZUMI, *Information geometry connecting Wasserstein distance and Kullback–Leibler divergence via the entropy-relaxed transportation problem*, Information Geometry, 1 (2018), pp. 13–37.
- [4] S.-I. AMARI AND T. MATSUDA, *Information geometry of Wasserstein statistics on shapes and affine deformations*, arXiv preprint arXiv:2307.12508, (2023).
- [5] S.-I. AMARI AND H. NAGAOKA, *Methods of information geometry*, vol. 191, American Mathematical Soc., 2000.
- [6] V. ARNOLD, *Sur la géométrie différentielle des groupes de lie de dimension infinie et ses applications à l'hydrodynamique des fluides parfaits*, in Annales de l'institut Fourier, vol. 16, 1966, pp. 319–361.
- [7] N. AY, J. JOST, H. VÂN LÊ, AND L. SCHWACHHÖFER, *Information geometry*, vol. 64, Springer, 2017.
- [8] G. E. BARTER AND D. L. DARMOFAL, *Shock capturing with pde-based artificial viscosity for dgfm: Part i. formulation*, Journal of Computational Physics, 229 (2010), pp. 1810–1827.
- [9] A. BHAGATWALA AND S. K. LELE, *A modified artificial viscosity approach for compressible turbulence simulations*, Journal of computational physics, 228 (2009), pp. 4965–4969.
- [10] H. BHAT AND R. FETEAU, *On a regularization of the compressible Euler equations for an isothermal gas*, Journal of mathematical analysis and applications, 358 (2009), pp. 168–181.
- [11] H. BHAT AND R. FETEAU, *The Riemann problem for the leray–burgers equation*, Journal of Differential Equations, 246 (2009), pp. 3957–3979.
- [12] H. S. BHAT AND R. C. FETEAU, *A Hamiltonian regularization of the Burgers equation*, Journal of Nonlinear Science, 16 (2006), pp. 615–638.
- [13] D. BODONY AND A. FIKL, *Adjoint-based sensitivity of shock-laden flows*, (2022).
- [14] Y. BRENIER, *The least action principle and the related concept of generalized flows for incompressible perfect fluids*, Journal of the American Mathematical Society, 2 (1989), pp. 225–255.
- [15] O. P. BRUNO, J. S. HESTHAVEN, AND D. V. LEIBOVICI, *Fc-based shock-dynamics solver with neural-network localized artificial-viscosity assignment*, Journal of Computational Physics:

- X, 15 (2022), p. 100110.
- [16] S. BUBECK, *Convex optimization: Algorithms and complexity*, Foundations and Trends in Machine Learning, 8 (2015), pp. 231–357.
 - [17] M. BURGER, M. ERBAR, F. HOFFMANN, D. MATTHES, AND A. SCHLICHTING, *Covariance-modulated optimal transport and gradient flows*, arXiv preprint arXiv:2302.07773, (2023).
 - [18] D. CHRISTODOULOU, *The formation of shocks in 3-dimensional fluids*, vol. 2, European Mathematical Society, 2007.
 - [19] D. CHRISTODOULOU, *The shock development problem*, 2019.
 - [20] D. CHRISTODOULOU AND S. KLAINERMAN, *The global nonlinear stability of the minkowski space*, Séminaire Équations aux dérivées partielles (Polytechnique) dit aussi” Séminaire Goulaouic-Schwartz”, (1993), pp. 1–29.
 - [21] D. CHRISTODOULOU AND S. MIAO, *Compressible flow and Euler’s equations*, vol. 9, International Press Somerville, MA, 2014.
 - [22] D. CLAMOND AND D. DUTYKH, *Non-dispersive conservative regularisation of nonlinear shallow water (and isentropic Euler equations)*, Communications in Nonlinear Science and Numerical Simulation, 55 (2018), pp. 237–247.
 - [23] A. W. COOK AND W. H. CABOT, *Hyperviscosity for shock-turbulence interactions*, Journal of Computational Physics, 203 (2005), pp. 379–385.
 - [24] V. DOLEŽÍ, M. FEISTAUER, AND C. SCHWAB, *On some aspects of the discontinuous galerkin finite element method for conservation laws*, Mathematics and Computers in Simulation, 61 (2003), pp. 333–346.
 - [25] D. G. EBIN AND J. MARSDEN, *Groups of diffeomorphisms and the motion of an incompressible fluid*, Annals of Mathematics, (1970), pp. 102–163.
 - [26] L. C. EVANS, *Partial differential equations*, vol. 19, American Mathematical Society, 2022.
 - [27] B. FIORINA AND S. K. LELE, *An artificial nonlinear diffusivity method for supersonic reacting flows with shocks*, Journal of Computational Physics, 222 (2007), pp. 246–264.
 - [28] F. GAY-BALMAZ AND H. YOSHIMURA, *A Lagrangian variational formulation for nonequilibrium thermodynamics. part i: discrete systems*, Journal of Geometry and Physics, 111 (2017), pp. 169–193.
 - [29] F. GAY-BALMAZ AND H. YOSHIMURA, *A Lagrangian variational formulation for nonequilibrium thermodynamics. part ii: continuum systems*, Journal of Geometry and Physics, 111 (2017), pp. 194–212.
 - [30] F. GAY-BALMAZ AND H. YOSHIMURA, *From Lagrangian mechanics to nonequilibrium thermodynamics: a variational perspective*, Entropy, 21 (2018), p. 8.
 - [31] B. GUELMAME, D. CLAMOND, AND S. JUNCA, *Hamiltonian regularisation of the unidimensional barotropic Euler equations*, Nonlinear Analysis: Real World Applications, 64 (2022), p. 103455.
 - [32] J.-L. GUERMOND, R. PASQUETTI, AND B. POPOV, *Entropy viscosity method for nonlinear conservation laws*, Journal of Computational Physics, 230 (2011), pp. 4248–4267.
 - [33] J.-L. GUERMOND AND B. POPOV, *Viscous regularization of the Euler equations and entropy principles*, SIAM Journal on Applied Mathematics, 74 (2014), pp. 284–305.
 - [34] A. HARTEN, B. ENGQUIST, S. OSHER, AND S. R. CHAKRAVARTHY, *Uniformly high order accurate essentially non-oscillatory schemes, III*, Journal of computational physics, 131 (1997), pp. 3–47.
 - [35] R. JORDAN, D. KINDERLEHRER, AND F. OTTO, *The variational formulation of the Fokker-Planck equation*, SIAM journal on mathematical analysis, 29 (1998), pp. 1–17.
 - [36] S. KAWAI, S. K. SHANKAR, AND S. K. LELE, *Assessment of localized artificial diffusivity scheme for large-eddy simulation of compressible turbulent flows*, Journal of computational physics, 229 (2010), pp. 1739–1762.
 - [37] B. KEITH AND T. M. SUROWIEC, *Proximal galerkin: A structure-preserving finite element method for pointwise bound constraints*, arXiv preprint arXiv:2307.12444, (2023).
 - [38] B. KHESIN AND G. MISIOLEK, *Shock waves for the burgers equation and curvatures of diffeomorphism groups*, Proceedings of the Steklov Institute of Mathematics, 259 (2007), p. 73.
 - [39] B. KHESIN, G. MISIOLEK, AND K. MODIN, *Geometric hydrodynamics and infinite-dimensional newton’s equations*, Bulletin of the American Mathematical Society, 58 (2021), pp. 377–442.
 - [40] J. LERAY, *Essai sur le mouvement d’un fluide visqueux emplissant l’espace*, Acta Math., 63 (1934), pp. 193–248.
 - [41] R. J. LEVEQUE AND R. J. LEVEQUE, *Numerical methods for conservation laws*, vol. 214, Springer, 1992.
 - [42] W. LI AND J. ZHAO, *Wasserstein information matrix*, Information Geometry, (2023), pp. 1–53.
 - [43] X.-D. LIU, S. OSHER, AND T. CHAN, *Weighted essentially non-oscillatory schemes*, Journal of computational physics, 115 (1994), pp. 200–212.

- [44] C. LOZANO, *Watch your adjoints! Lack of mesh convergence in inviscid adjoint solutions*, AIAA Journal, 57 (2019), pp. 3991–4006.
- [45] A. MANI, J. LARSSON, AND P. MOIN, *Suitability of artificial bulk viscosity for large-eddy simulation of turbulent flows with shocks*, Journal of Computational Physics, 228 (2009), pp. 7368–7374.
- [46] A. S. NEMIROVSKI AND M. J. TODD, *Interior-point methods for optimization*, Acta Numerica, 17 (2008), pp. 191–234.
- [47] A. S. NEMIROVSKI AND D. B. YUDIN, *Problem complexity and method efficiency in optimization*, (1983).
- [48] Y. E. NESTEROV, M. J. TODD, ET AL., *On the Riemannian geometry defined by self-concordant barriers and interior-point methods*, Foundations of Computational Mathematics, 2 (2002), pp. 333–361.
- [49] G. PEYRÉ, M. CUTURI, ET AL., *Computational optimal transport: With applications to data science*, Foundations and Trends® in Machine Learning, 11 (2019), pp. 355–607.
- [50] G. PUPPO, *Numerical entropy production for central schemes*, SIAM Journal on Scientific Computing, 25 (2004), pp. 1382–1415.
- [51] D. RAY AND J. S. HESTHAVEN, *An artificial neural network as a troubled-cell indicator*, Journal of computational physics, 367 (2018), pp. 166–191.
- [52] A. SCHMEDING, *An Introduction to Infinite-Dimensional Differential Geometry*, Cambridge Studies in Advanced Mathematics, Cambridge University Press, 2022, <https://doi.org/10.1017/9781009091251>.
- [53] C.-W. SHU, *Advanced numerical approximation of nonlinear hyperbolic equations, chapter essentially non-oscillatory and weighted essentially non-oscillatory schemes for hyperbolic conservation laws*, 1998.
- [54] T. C. SIDERIS, *Formation of singularities in three-dimensional compressible fluids*, Communications in mathematical physics, 101 (1985), pp. 475–485.
- [55] B. VAN LEER, *Towards the ultimate conservative difference scheme. V. a second-order sequel to godunov’s method*, Journal of computational Physics, 32 (1979), pp. 101–136.
- [56] J. VONNEUMANN AND R. D. RICHTMYER, *A method for the numerical calculation of hydrodynamic shocks*, Journal of applied physics, 21 (1950), pp. 232–237.
- [57] H. YOSHIMURA AND F. GAY-BALMAZ, *Hamiltonian variational formulation for non-simple thermodynamic systems*, in International Conference on Geometric Science of Information, Springer, 2023, pp. 221–230.